A PHYSICS-INFORMED NEURAL NETWORK FRAMEWORK FOR CHARACTERIZATION OF DAMAGE IN COMPOSITES

Abouali, S. [1]*, Haghighat, E.[1], Vaziri, R.[1]
[1] Composites Research Network (CRN), Departments of Civil Engineering and Materials Engineering, The University of British Columbia, Vancouver, Canada
* Corresponding author (sahar@composites.ubc.ca)

Keywords*: Damage characterization, Machine learning, Physics-informed neural networks*

ABSTRACT

For true simulation of the mechanical behavior of a material by a phenomenological constitutive model, the parameters of the model should be characterized effectively and accurately. In this work, we propose a physics-informed neural network (PINN) framework to characterize the damage behavior of composites based on a limited set of data acquired from the local zone of damage. For development of the proposed framework, the fracture process zone in an over-height compact tension (OCT) test setup is considered as the damage domain of interest and a PINN is tailored to this setup for inverse analysis in order to characterizate the constitutive parameters. Governing principles such as the constitutive relations and equilibrium equations are incorporated in the loss function of the PINN. The proposed framework is validated by characterization of parameters of a coupled damage-plasticity material model applied to simulation of the response of a quasi-isotropic composite laminate.

1 INTRODUCTION

With ongoing development of nonlinear and complex constitutive models for simulating damage in composite materials, it is imperative to efficiently characterize (identify) the material parameters used in these constitutive models. In order to identify the parameters of a constitutive model, inverse analyses have been frequently used in the literature e.g. [1]–[3]. Most inverse analyses require repetitive forward simulations. In these methods, input material parameters in the simulations are adjusted by optimization of an objective function in an iterative procedure to reproduce the experimental results.

For application of a physics-based macroscopic damage model of composite, characterization of the strain-softening law is needed in addition to initial elastic properties and strength values e.g. [4]. For the construction of strain-softening curve of the laminate, Zobeiry et al. [5] developed a method based on performing over-height compact tension (OCT) and compact compression (CC) experiments combined with using Digital Image Correlation (DIC) technique for recording full-field displacement along the specimen surface. Damage boundaries and initiation strain are identified by checking local equilibrium conditions at virtual nodes, and strain-softening curves are then constructed by making certain assumptions about average stress and strain within the damage zone based on those values at the boundary between the damaged and elastic (undamaged) regions. Despite adoption of inverse methods, in this work there is no prior assumption on the shape of the strain-softening curve, however, a complex data analysis scheme is required and the assumptions associated with the calculation of stress and strain in the damage zone may lead to loss of accuracy.

Rapid development of data-driven models as the fourth scientific paradigm and availability of deep learning software such as Tensorflow [6] have prompted their application to constitutive modeling and characterization e.g. [7], [8]. In a recent study on the application of theory-guided machine learning in damage of composites, a neural network model has been developed for the characterization of the tensile damage in composites [9]. This

model, that is trained by 10,000 FE simulations, approximates the damage parameters based on the experimentally measured force-displacement data. This approach helps to characterize damage with reduced experimental effort. However, the training of the neural networks is data demanding and requires conducting many high-fidelity and robust FE simulations.

Physics-informed neural networks (PINN), see for example [10], [11] among others, are alternative methods in machine learning for incorporating the prior knowledge of the problem into the neural network algorithm. For this purpose, the prior knowledge of the system, that can be physical laws, constitutive relationships or empirical governing rules, are formulated into the loss functions. PINNs have been used as new classes of numerical solvers for PDEs, e.g. [12]. PINN can also be used in solving inverse problems to identify the unknown parameters. Haghighat et al. [13] have demonstrated application of PINNs for identification of Lame's constants of an isotropic elastic material under plane-strain conditions.

In this work, we present a physics-informed neural network framework for characterization of tensile damage parameters of composites. The constitutive model that is studied for this purpose is a coupled damage-plasticity model. It should be noted that although this particular constitutive model is employed in this study, the proposed framework can be adapted to other forms of constitutive models.

2 Methodology for damage characterization

2.1 Constitutive model

Several damage models based on both discrete and continuum approaches have been developed in the literature. In this work, for simulation of the highly nonlinear damage response of composite laminates, an isotropic coupled damage-plasticity constitutive model is adopted. In this model, elasto-plastic constitutive relations are formulated in the effective stress space defined as [14]:

$$\tilde{\boldsymbol{\sigma}} = \frac{\boldsymbol{\sigma}}{1-\omega} \tag{1}$$

where $\boldsymbol{\sigma}$ is the Cauchy stress tensor representing the actual state of stress in the damaged material and $\tilde{\boldsymbol{\sigma}}$ is the effective stress tensor representing the state of stress in an equivalent undamaged material subject to the same strain state. ω denotes the isotropic scalar damage variable, which varies between 0 and 1.

The elasto-plastic model is defined using a von-Mises yield criterion and associated plastic flow rule with no hardening. The rate form of the elasto-plastic constitutive relations can be expressed as:

$$\dot{\boldsymbol{\sigma}} = (1-\omega)\boldsymbol{C}:\left(\dot{\boldsymbol{\epsilon}} - \dot{\boldsymbol{\epsilon}}^{\boldsymbol{p}}\right) - \dot{\omega}\boldsymbol{C}:(\boldsymbol{\epsilon} - \boldsymbol{\epsilon}^{\boldsymbol{p}}) \tag{2}$$

where $\boldsymbol{C}$ is the fourth-order elastic stiffness operator defined in terms of the material's elastic modulus E and Poisson's ratio ν. $\boldsymbol{\epsilon}^{\boldsymbol{p}}$ is the plastic strain tensor that can be determined according to the normality hypothesis. In this model, the damage variable ω should be defined as a function of equivalent plastic strain $\bar{\epsilon}_p$. For the purposes of this study, damage growth is considered as a linear function of the equivalent plastic strain that results in a linear strain-softening response. Also, it is assumed that plasticity and damage initiate simultaneously:

$$\omega = \frac{\bar{\epsilon}_p}{\bar{\epsilon}_{ps}} \qquad 0 < \bar{\epsilon}_p < \bar{\epsilon}_{ps} \tag{3}$$

where $\bar{\epsilon}_{ps}$ represents the equivalent plastic strain at damage saturation that is referred to as damage saturation strain in the rest of this paper. The schematic of this damage evolution curve and corresponding stress-strain curve under uniaxial loading condition is shown in Figure 1. The material parameters that are to be characterized for this model are elastic modulus E, Poisson's ratio ν, peak (yield) stress σ_i and damage saturation strain $\bar{\epsilon}_{ps}$. It is worth noting that any general shape other than the bilinear shape shown here for the stress-strain curve can be implemented in this constitutive model.

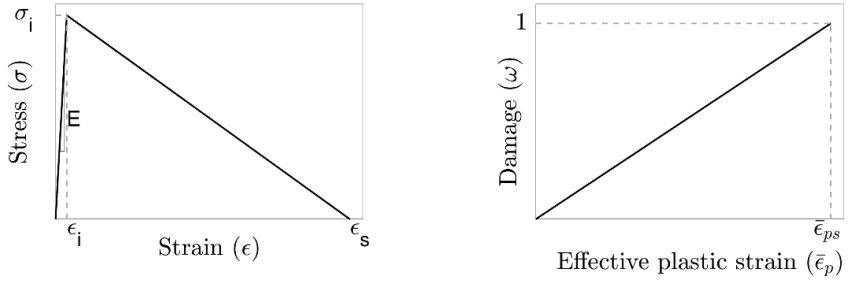

Figure 1. Coupled damage-plasticity material model : stress-strain curve (left) and damage-effective plastic strain curve (right)

2.2 Test set up for damage characterization

It is important to have a testing configuration/domain that promotes a stable growth of damage in a given composite laminate to trigger a softening response and generate enough data in the strain-softening regime of the material. To this end, the over-height compact tension (OCT) test developed by Kongshavn and Poursartip [15] is adopted here (Figure 2). For the current characterization approach, the data that needs to be collected from this test include the time histories of the applied force (F) and strain in the zone of interest Ω that lies ahead of the notch as shown in Figure 2.

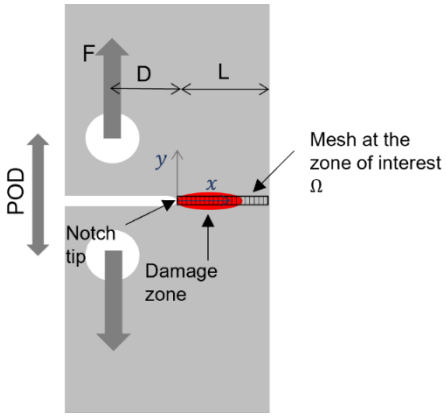

Figure 2. Over-height compact tension (OCT) test used for data generation

2.3 PINN solver

Building upon the proposed solver for elasto-plastic constitutive models described in [16], a PINN model is tailored to the OCT setup. Similar to [16], in order to solve the nonlinear system of ODEs of plasticity, the plastic multiplier, γ is approximated by a neural network as a continuous function of time t. Here, as there is no direct measurement of the stress field $\boldsymbol{\sigma}$, it is also approximated by the same neural network. For the current plane stress setup, the stress field $\boldsymbol{\sigma}$ is expressed as:

$$\boldsymbol{\sigma} = \begin{bmatrix} \sigma_{xx} & \sigma_{xy} \\ \sigma_{xy} & \sigma_{yy} \end{bmatrix} \tag{4}$$

The constructed neural network can be represented as:

$$(\gamma, \boldsymbol{\sigma}) \approx (\hat{\gamma}, \hat{\boldsymbol{\sigma}}) = \mathcal{N}(t; \boldsymbol{\theta}, \boldsymbol{\lambda}) \tag{5}$$

where, t is the input to the neural network, $\mathcal{N}$ denotes the feed-forward neural network, $\boldsymbol{\theta}$ represents the network parameters (weights and biases), $\boldsymbol{\lambda}$ denotes the vector of material parameters, and $(\hat{\gamma}, \hat{\boldsymbol{\sigma}})$ are the

approximated plastic multiplier and stress tensor in the zone of interest. The parameters of the neural network $\boldsymbol{\theta}$ and the unknown material parameters $\boldsymbol{\lambda}$ can be learned simultaneously by minimizing a loss function that represents the error in the network's predictions.

The loss function in the PINN, $\mathcal{L}$, is the summation of losses associated with any prior knowledge $\mathcal{L}_{prior}$ and losses associated with the training data $\mathcal{L}_{data}$:

$$\mathcal{L} = \mathcal{L}_{prior} + \mathcal{L}_{data} \tag{6}$$

The physics of the problem is governed by global equilibrium of force and moment when taking a through thickness cross-section at the fracture process zone ahead of the notch as shown in Figure 3. These equilibrium equations can be considered as constraints that should be embedded in the $\mathcal{L}_{prior}$:

$$F - b\int_0^L \hat{\sigma}_{yy} dx = 0 \tag{7}$$

$$F.D - b\int_0^L \hat{\sigma}_{yy} x dx = 0 \tag{8}$$

where *b* is the thickness of the laminate.

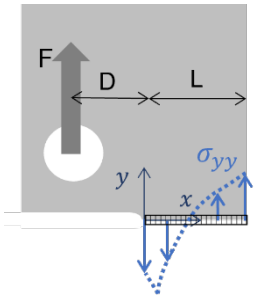

Figure 3. Free body diagram of the OCT specimen used for equilibrium constraints

For the calculation of the integrals in the above equations, with inspiration from FE, the spatial domain Ω is discretized into elements, and Gauss quadrature points in each element are used for integration. Loss terms corresponding to the equilibrium constraints are written in terms of mean squared error (MSE):

$$\mathcal{L}_F = \frac{1}{n}\sum_{i=1}^{n}\left(F|_{t_i} - b\int_0^L \hat{\sigma}_{yy} dx\,|_{t_i}\right)^2 \qquad t_i \in [0,T] \tag{9}$$

$$\mathcal{L}_M = \frac{1}{n}\sum_{i=1}^{n}\left(F.D|_{t_i} - b\int_0^L \hat{\sigma}_{yy} x dx\,|_{t_i}\right)^2 \qquad t_i \in [0,T] \tag{10}$$

where t_i represent the time steps at which external force F and neural network outputs $\hat{\gamma}, \hat{\boldsymbol{\sigma}}$ are sampled and *n* is the total number of datapoints.

Constitutive relationships are another key prior. Here, the general form of ODEs associated with the constitutive relations at one integration point, is represented as $g\left(\boldsymbol{\epsilon}, \dot{\boldsymbol{\epsilon}}, \hat{\gamma}, \hat{\boldsymbol{\sigma}}, \dot{\hat{\gamma}}, \dot{\hat{\boldsymbol{\sigma}}}, \boldsymbol{\lambda}\right) = 0$. For a detailed review of these constraints one may refer to Table 1 in [16]. The material parameters that are to be predicted are collected into one vector denoted as $\boldsymbol{\lambda} = \left[E, \nu, \sigma_i, \bar{\epsilon}_{ps}\right]$. The residuals of these ODEs are considered as the constraints and the MSE loss terms for the constitutive ODEs is then given by:

$$\mathcal{L}_c = \frac{1}{n}\sum_{i=1}^{n}\left(g\left(\boldsymbol{\epsilon}, \dot{\boldsymbol{\epsilon}}, \hat{\gamma}, \hat{\boldsymbol{\sigma}}, \dot{\hat{\gamma}}, \dot{\hat{\boldsymbol{\sigma}}}, \boldsymbol{\lambda}\right)|_{t_i}\right)^2 \qquad t_i \in [0,T] \tag{11}$$

It is worth noting that the loss terms for the constitutive model include time derivatives (a.k.a. rates) of the neural network approximations of $\hat{\gamma}, \hat{\boldsymbol{\sigma}}$; these derivatives are computed using the available technology for "automatic differentiation" in TensorFlow.

The initial conditions for constitutive ODEs for one integration point are written as :

$$\hat{\gamma}|_{t=0} = \gamma_0 \tag{12}$$

$$\hat{\boldsymbol{\sigma}}|_{t=0} = \boldsymbol{\sigma_0} \tag{13}$$

where γ_0 , $\boldsymbol{\sigma_0}$ are the initial condition for the plastic multiplier and stress. The loss term associated with initial conditions for one integration point are defined as:

$$\mathcal{L}_{\gamma_0} = \hat{\gamma}|_{t=0} - \gamma_0 \tag{14}$$

$$\mathcal{L}_{\boldsymbol{\sigma_{0_0}}} = \hat{\boldsymbol{\sigma}}|_{t=0} - \boldsymbol{\sigma_0} \tag{15}$$

Finally, the total loss is the summation of two equilibrium loss terms (9, 10), constitutive loss terms (11) and initial value loss terms (14, 15), summed over all integration points:

$$\mathcal{L} = \mathcal{L}_F + \mathcal{L}_M + \sum_{m=1}^{M} (\mathcal{L}_c)_m + (\mathcal{L}_{\gamma_0})_m + (\mathcal{L}_{\boldsymbol{\sigma_{0_0}}})_m \tag{16}$$

where M is the total number of integration points in the spatial domain.

After construction of the network, it should be trained using data. The data needed for training of this network include time history of force F, time history of strain in the domain, x coordinates of the integration points and initial values of the stress field and plastic multiplier. The network is then trained on these sets of data by minimizing the total loss with respect to the network parameters $\boldsymbol{\theta}, \boldsymbol{\lambda}$:

$$(\boldsymbol{\theta}_{opt}, \boldsymbol{\lambda}_{opt}) = \underset{\boldsymbol{\theta},\boldsymbol{\lambda}}{\operatorname{argmin}}\, \mathcal{L} \tag{17}$$

After the training, the plastic multiplier and stress field are approximated, and the material parameters are identifed.

The PINN is encoded in a high-level Keras wrapper called SciANN [17], that is specifically developed for physics-informed deep learning and scientific computations. The adopted neural network has 8 hidden layers and 20 neurons per layer. A hyperbolic-tangent function is selected as the activation function of the hidden layers due to its smoothness and non-zero derivative. A full-batch optimization scheme is used together with Adam optimizer [18].

3 Case study

To assess the performance of the proposed framework, it is applied to the characterization of parameters of the coupled damage-plasticity model described in Section 2.1. As a validation step, the PINN is first used to determine the constitutive model parameters for a single-element setup, as presented in Appendix A. It can be seen from Table A.1, that the PINN framework is able to characterize the damage-plasticity parameters quite accurately. This instils confidence in applying the developed PINN to a more complex loading geometry. In the following, we investigate the application of the PINN to characterization of the constitutive model parameters of a composite specimen subjected to OCT testing.

To avoid the complexities of dealing with experimental data at this stage, the required data are synthetically generated by performing FE simulation of the OCT test on quasi-isotropic IM7/8552 CFRP laminate. The constitutive parameters used for performing the FE simulation are $E = 60\ GPa, \nu = 0.32, \sigma_i = 663, \bar{\epsilon}_{ps} = 0.29$ that are based on the work by Zobeiry et al. [5]. The data generated by the FE analysis used for training of the PINN, are time histories of the applied force (F) and all strain components in the zone of interest, Ω. For

evaluation of the integrals in equilibrium loss terms, a uniform mesh with 46 Gaussian integration points on spatial domain along x (as shown in Figure 3) is used.

To facilitate the inverse analysis, elastic parameters E, ν are firstly identified by training the PINN using the data at early stages of loading when the material behavior is elastic. A total number of 40 datapoints are uniformly sampled on $t \in [0.0\ , 1.6]$ seconds. Training data for identification of the elastic parameters are represented in Figure 4.

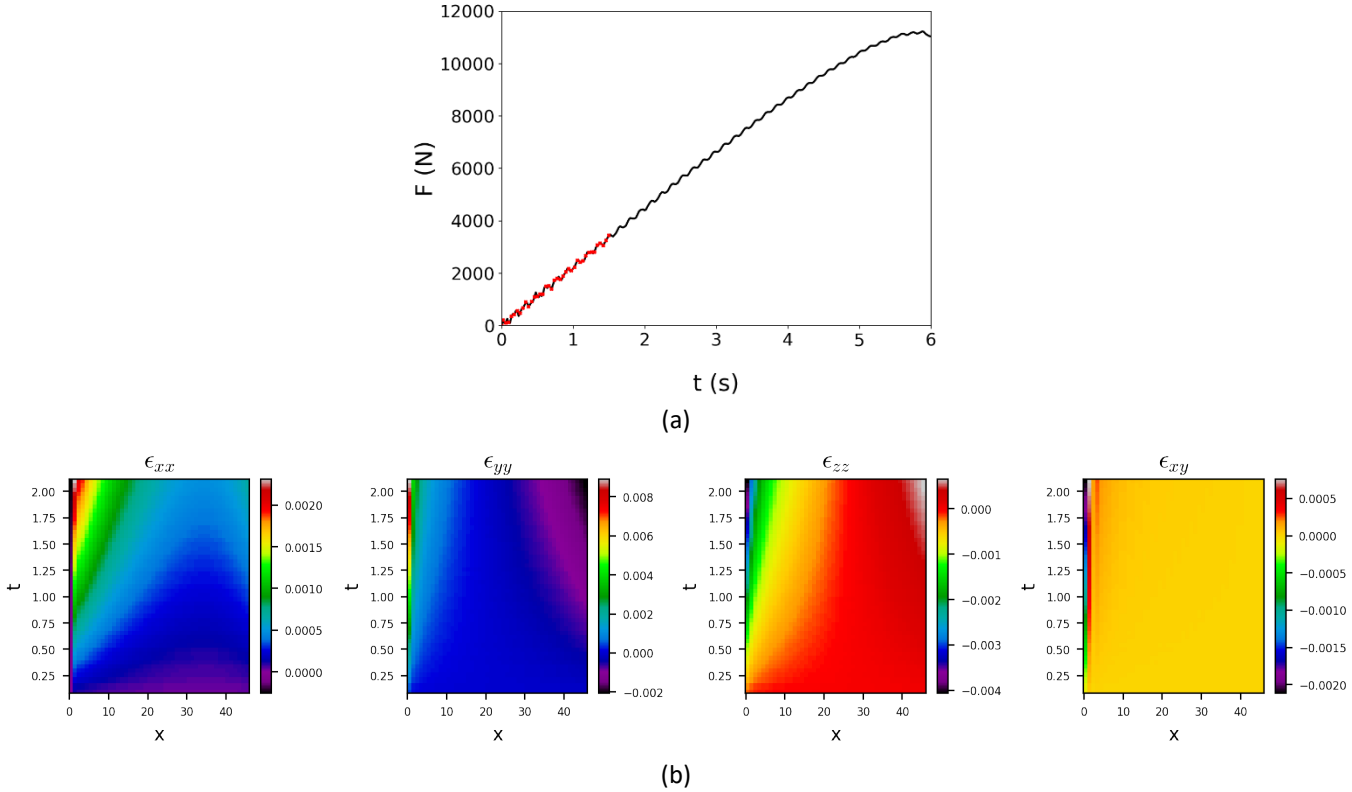

Figure 4. Training data used for identification of the elastic parameters E and ν: (a) sampled force vs time (sampled datapoints are marked in red), and (b) sampled strain in the zone of interest

After the elastic parameters are identified, damage parameters $\sigma_i, \bar{\epsilon}_{ps}$ are characterized by training the PINN on the data sampled later in time when nonlinear behavior due to plasticity and damage have likely emerged. A total number of 110 datapoints are uniformly sampled on $t \in [1.6\ , 5.9]$ seconds. Training data for identification of the damage parameters are represented in Figure 4.

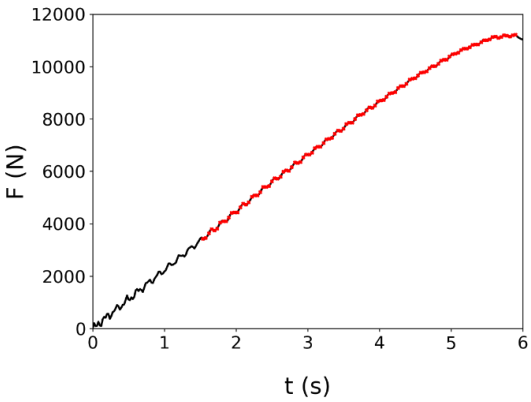

(a)

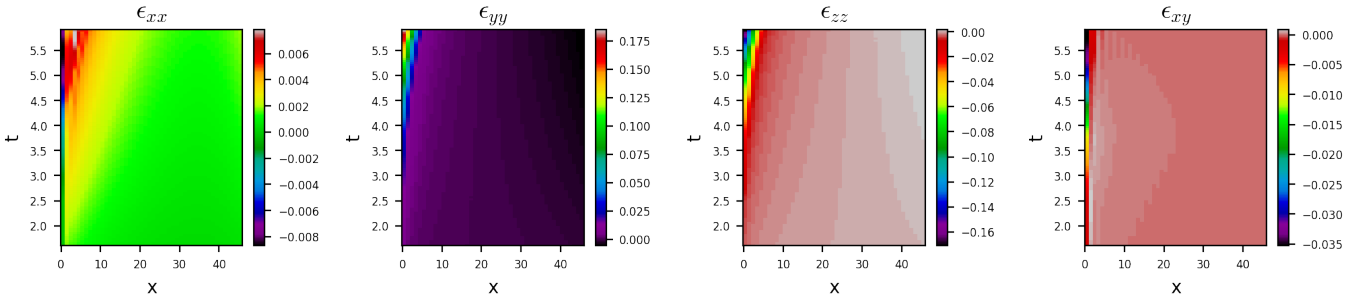

(b)

Figure 5. Training data used for identification of the damage parameters σ_i and $\bar{\epsilon}_{ps}$: (a) sampled force vs time (sampled datapoints are marked in red), and (b) sampled strain in the zone of interest

Results and discussion

After training the proposed PINN model using the force and strain data, the plastic multiplier and stress field in the domain of interest are approximated and the material parameters are identified. The predicted parameters are compared to the ground truth values in Table 1. The error for each parameter in this table is calculated as:

$$\text{Error} = \frac{|\ \text{PINN Predicted}\ -\ \text{Ground truth}|}{\text{Ground truth}} \tag{18}$$

Table 1. Characterized parameters based on the OCT test geometry

Parameter	PINN Predicted	Ground truth	Error %
Elastic modulus, E (GPa)	58	60	3
Poisson's ratio, ν	0.32	0.32	0
Peak stress, σ_i (MPa)	612	663	8
Damage saturation strain, $\bar{\epsilon}_{ps}$	0.43	0.29	48

The resulting characterized stress-strain curve is plotted and compared to the ground truth stress-strain curve used for data generation in Figure 6(a). The fracture energy of the material can be calculated based on the area below the stress-strain curve. For the 1 mm finite element mesh size used in this study, this value is 168 kJ/m^2.
From Table 1and Figure 6(a), it can be seen that with the exception of the damage saturation strain, the prediction error for all other parameters is relatively small. We speculate that the large error in the damage saturation strain is due to the fact that this parameter is less pronounced in the pre-peak data of the force-time curve used as training data in this study. To assess this idea, PINN-characterized stress-strain curve is used as input for simulation of the OCT test using LS-DYNA and the resulting force-time curve is compared to the corresponding training data. Figure 6(b) shows this comparison to be fair for the pre-peak region of the force-time curve. From this observation it can be inferred that with the given pre-peak training data, the model performs reasonably well and that the error in prediction of the damage saturation strain can be attributed to the absence of training data in the post-peak regime of the force-time curve. In fact, in the single element study presented in Appendix A, it is shown that when data from the post-peak regime of force-time curve are included in training, the damage saturation strain can be accurately predicted. Work is currently underway to incorporate the post-peak training data as this requires further modifications to the PINN model to handle the high level of noise that is inherent in explicit FE analysis involving fully damaged elements (i.e. elements that have exceeded damage saturation strain).

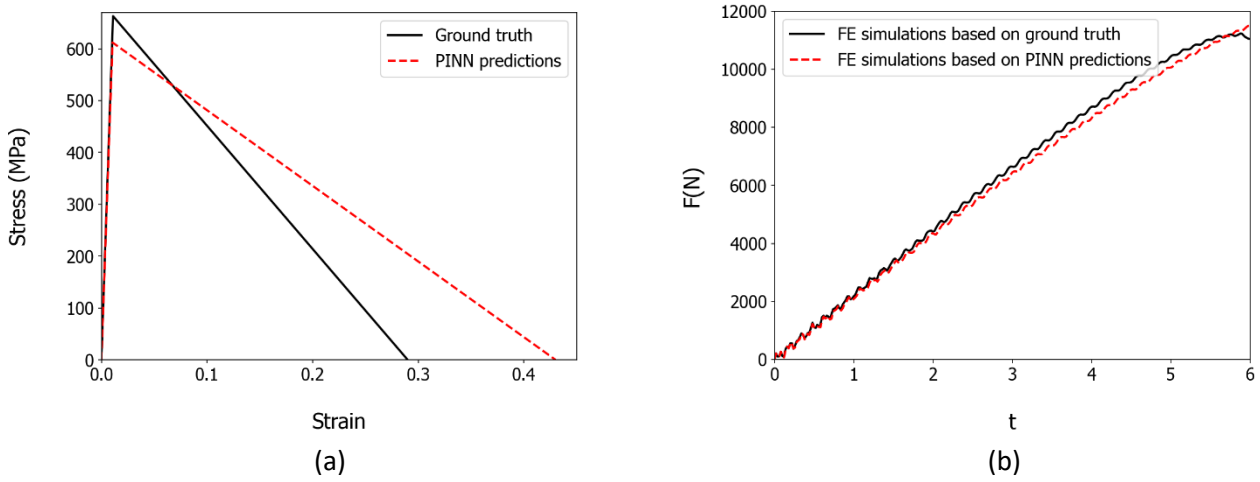

Figure 6. (a) Comparison of PINN characterized stress-strain curve and the ground truth (b) comparison of the force-time curves obtained from LS-DYNA based on ground truth and PINN predicted stress-strain curves as input

4 Conclusion

We present a physics-informed neural network (PINN) framework for damage characterization of composites. The proposed model only uses external force and field strains as training data. Performance of this PINN model has been demonstrated for characterization of material parameters of a coupled damage-plasticity constitutive model applied to simulation of a quasi-isotropic composite laminate. In this study, data needed for training of the PINN are extracted from FE simulations of OCT tests. Currently the PINN model can predict the elastic parameters and the peak stress (or damage initiation strain) fairly well, however, it is shown that for accurate prediction of the damage saturation strain parameter data from the post-peak regime of the OCT test should be included in the training. This regime accompanies sudden fracturing behavior that lead to high level of noise in local strain data. Future research efforts will focus on dealing with the nosiy data when postpeak regime is considered for training the PINN.

Appendix A. Validation of the proposed framework by characterization of the constitutive model parameters for a single element setup

To verify the effectiveness of the PINN predictions for coupled damage-plasticity characterization, we have conducted a single element analysis under uniaxial loading that follows the force-time history shown in Figure A.1. The generated data including force and strain-time histories were used for training the PINN. The predicted damage parameters by the PINN are listed in Table A.1. It can be seen that the PINN framework is able to characterize the damage-plasticity parameters for this setup quite accurately. It should be noted that the training data were sampled from both pre-peak and post-peak regimes in force-time history but noisy data after damage saturation were not included in the training data.

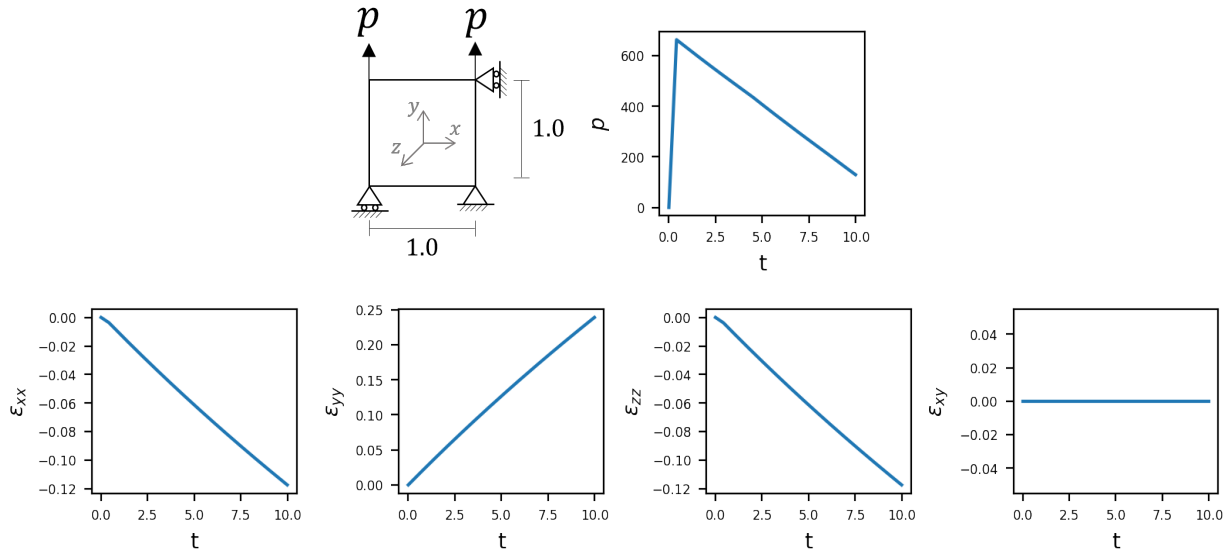

Figure A.1. Single element and the training data which includes the post-peak regime used for identification of the damage parameters

Table A.1. Characterized parameters based on the single element model where post peak data are used in addition to pre-peak data for training

Parameter	PINN Predicted	Ground truth	Error %
Elastic modulus, E (GPa)	62	60	3.3
Poisson's ratio, ν	0.32	0.32	0
Peak stress, σ_i (MPa)	640	663	3.5
Damage saturation strain, $\bar{\epsilon}_{ps}$	0.29	0.29	0

References

[1] P. A. Prates, A. F. G. Pereira, N. A. Sakharova, M. C. Oliveira, and J. V. Fernandes, "Inverse Strategies for Identifying the Parameters of Constitutive Laws of Metal Sheets," *Adv. Mater. Sci. Eng.*, vol. 2016, 2016.

[2] S. Cooreman, D. Lecompte, H. Sol, J. Vantomme, and D. Debruyne, "Elasto-plastic material parameter identification by inverse methods: Calculation of the sensitivity matrix," *Int. J. Solids Struct.*, vol. 44, no. 13, pp. 4329–4341, Jun. 2007.

[3] M. Grédiac and F. Pierron, "Applying the Virtual Fields Method to the identification of elasto-plastic constitutive parameters," *Int. J. Plast.*, vol. 22, no. 4, pp. 602–627, Apr. 2006.

[4] C. McGregor, N. Zobeiry, R. Vaziri, A. Poursartip, and X. Xiao, "Calibration and validation of a continuum damage mechanics model in aid of axial crush simulation of braided composite tubes," *Compos. Part A Appl. Sci. Manuf.*, vol. 95, pp. 208–219, 2017.

[5] N. Zobeiry, R. Vaziri, and A. Poursartip, "Characterization of strain-softening behavior and failure mechanisms of composites under tension and compression," *Compos. PART A*, vol. 68, pp. 29–41, 2015.

[6] "TensorFlow: A System for Large-Scale Machine Learning | USENIX." [Online]. Available: https://www.usenix.org/conference/osdi16/technical-sessions/presentation/abadi. [Accessed: 31-Mar-2022].

[7] Gdoutos, *Fracture mechanics*. 2021.

[8] C. Yang, Y. Kim, S. Ryu, and G. X. Gu, "Prediction of composite microstructure stress-strain curves using convolutional neural networks," *Mater. Des.*, vol. 189, Apr. 2020.

[9] N. Zobeiry, J. Reiner, and R. Vaziri, "Theory-Guided Machine Learning for Damage Characterization of Composites," *Compos. Struct.*, p. 112407, 2020.

[10] M. Raissi, P. Perdikaris, and G. E. Karniadakis, "Physics-informed neural networks: A deep learning framework for solving forward and inverse problems involving nonlinear partial differential equations," *J. Comput. Phys.*, vol. 378, pp. 686–707, 2019.

[11] K. Shukla, A. D. Jagtap, and G. E. Karniadakis, "Parallel physics-informed neural networks via domain decomposition," *J. Comput. Phys.*, vol. 447, p. 110683, Dec. 2021.

[12] D. Zhang, L. Lu, L. Guo, and G. E. Karniadakis, "Quantifying total uncertainty in physics-informed neural networks for solving forward and inverse stochastic problems," *J. Comput. Phys.*, vol. 397, p. 108850, Nov. 2019.

[13] E. Haghighat, M. Raissi, A. Moure, H. Gomez, and R. Juanes, "A physics-informed deep learning framework for inversion and surrogate modeling in solid mechanics," *Comput. Methods Appl. Mech. Eng.*, vol. 379, p. 113741, Jun. 2021.

[14] L. M. Kachanov, "Rupture Time Under Creep Conditions," *Int. J. Fract. 1999 971*, vol. 97, no. 1, pp. 11–18, 1999.

[15] I. Kongshavn and A. Poursartip, "Experimental investigation of a strain-softening approach to predicting failure in notched fibre-reinforced composite laminates," *Compos. Sci. Technol.*, vol. 59, no. 1, 1999.

[16] E. Haghighat, S. Abouali, and R. Vaziri, "Constitutive model characterization and discovery using physics-informed deep learning," *arXiv Prepr. arXiv1604*, Mar. 2022.

[17] E. Haghighat and R. Juanes, "SciANN: A Keras/TensorFlow wrapper for scientific computations and physics-informed deep learning using artificial neural networks," *Comput. Methods Appl. Mech. Eng.*, vol. 373, p. 113552, Jan. 2021.

[18] D. P. Kingma and J. L. Ba, "Adam: A Method for Stochastic Optimization," *3rd Int. Conf. Learn. Represent. ICLR 2015 - Conf. Track Proc.*, Dec. 2014.